Cellulose (2019) 26:3255–3269
https://doi.org/10.1007/s10570-019-02263-w

ORIGINAL RESEARCH

Fabrication and performance characterization of the membrane from self-dispersed gelatin-coupled cellulose microgels

Yijun Yao · Hongru Wang · Ruirui Wang · Yong Chai · Wanli Ji

Received: 25 August 2018 / Accepted: 14 January 2019 / Published online: 18 January 2019

Abstract A new gelatin-coupled cellulose (GCC) microgel system was successfully prepared in NaOH/urea aqueous solution with epichlorohydrin (ECH) as a coupling agent via dialysis and self-dispersion pathway. The structure and property of the microgel and its membrane were characterized by elemental analysis, dynamic light scattering (DLS), Fourier transform infrared (FTIR) spectra, gel permeation chromatography (GPC), scanning electron microscopy (SEM), atomic force microscopy (AFM), X-ray diffraction (XRD) and thermogravimetric analysis (TGA). It was concluded that successful coupling interactions occurred between cellulose and gelatin during the fabrication process, and the weight-average molecular weight of GCC microgel was up to 636.60 kDa with polydispersity index (PDI) of 1.015 approximately. The crystalline structure of the modified cellulose was destroyed, leading to GCC product self-dispersed in water in the absence of NaOH and urea. The GCC microgels had whisker-like structure, and their Z-average particle sizes were approximately 86.1 nm–150.2 nm and decreased with the increases of the gelatin content (W_{Gel}). In comparison with the water contact angle, swelling behavior and thermostability of the existing water-soluble cellulose derivative, the microgel membranes exhibited better water resistance and thermal resistance properties.

Electronic supplementary material The online version of this article (https://doi.org/10.1007/s10570-019-02263-w) contains supplementary material, which is available to authorized users.

Y. Yao · H. Wang (✉) · R. Wang · Y. Chai · W. Ji
College of Bioresources Chemical and Materials Engineering, Shaanxi University of Science and Technology, Xi'an 710021, Shaanxi Province, China
e-mail: wanghr@sust.edu.cn

Graphical abstract

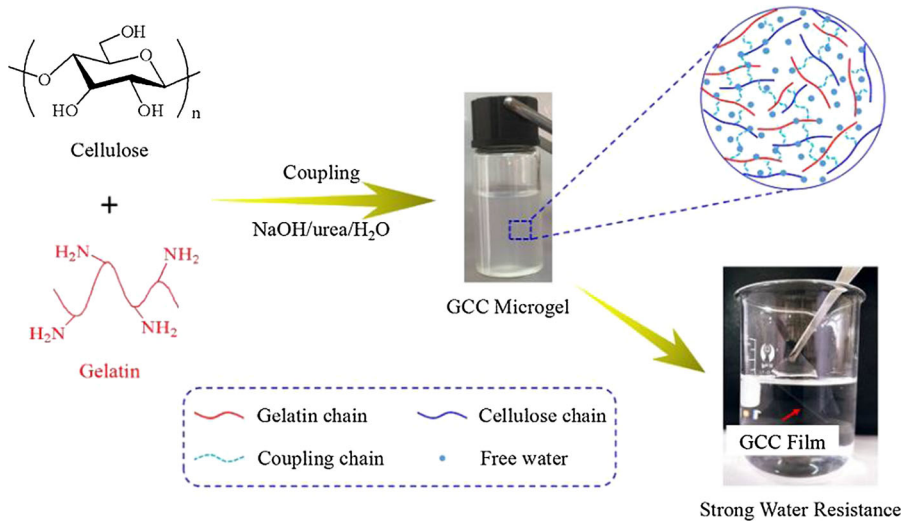

Keywords Gelatin-coupled cellulose · Microgel · Dialysis · Self-dispersion

Introduction

Cellulose is the most abundant renewable biopolymer, with an annual production volume of about 1.5×10^{12} t (Klemm et al. 2005; Tristram et al. 2015). Nowadays, functional materials based on cellulose have attracted considerable attention due to their biodegradability, low-cost, biocompatibility and ease of modify, etc. (Zhang et al. 2018a, b; Yang et al. 2017; Geng 2018; Sun et al. 2017). However, the strong hydrogen bond network structure in the intra- and inter-molecular of cellulose makes it insoluble in both water and general organic solvents, leading to considerable difficulties for the processing of cellulose based materials. Therefore, coatings based on cellulose body are very limited, and only the water dispersions of cellulose derivatives including cellulose acetate (CA) (Zhang and Weeks 2014; Su et al. 2017), nitrocellulose (NC) (Su et al. 2015; Ma et al. 2012), methylcellulose (MC) (Zhou et al. 2008), ethyl cellulose (EC) (Lu and Yuan 2018), quaternized cellulose (QC) (You et al. 2014; Song et al. 2008), hydroxyethyl cellulose (HEC) (Zhou et al. 2006), hydroxypropyl cellulose (HPC) (Zhou et al. 2004), carboxymethycellulose (CMC) (Qi et al. 2009), hydroxypropyl methylcellulose (HPMC) (Esteghlal et al. 2016), and carboxymethyl cellulose nitrate ester (CMCN) (Duan et al. 2016), etc., have been prepared and developed widely for a long time. Nevertheless, the plentiful potential applications of cellulose ethers are restricted by their low molecular weight and high hygroscopic properties, resulting in loss of mechanical properties and physical degradation. CA and NC coatings possess high transparency and emulsion stability, they can be dispersed in water by introducing polyurethane pre-polymer with hydrophilic groups to give a good film-forming property, whereas a large number of organic solvents need to be used in the waterborne process, in fact the total water emulsification is not achieved. In addition, NC has poor light resistance, yellowing, and the price of CA is high which limit their further extensive application.

With the emergence of new solvent systems for cellulose, such as ionic liquids (ILs) (Suzuki et al. 2014; Xia et al. 2016), *N*,*N*-dimethylacetamide/lithium chloride (DMAc/LiCl) (Qiu et al. 2012; Zhang et al. 2012) and NaOH/urea aqueous solution (Cai and Zhang 2005; Pei et al. 2013; Hu et al. 2015), etc., a series of graft copolymers which can be dissolved in common solvents was prepared via weakening the intra- and inter-molecular hydrogen bonding interactions of cellulose with chemical modification under homogeneous reaction condition, such as many amphiphilic cellulose copolymers including cellulose-graft-poly[2-(*N*,*N*-dimethyl amino) ethyl methacrylate] (cell-*g*-PDMAEMA) (Sui et al. 2008),

cellulose-graft-poly(*N*-isopropylacrylamide) (cell-*g*-PNIPAM) (Ifuku and Kadla 2009; Xu et al. 2010), cellulose-graft-poly(ε-caprolactone) (cell-*g*-PCL) (Guo et al. 2013), cellulose-graft-polydioxanone (cell-*g*-PDO) (Ge et al. 2015), and cellulose-graft-poly(glutamic acid) (cell-*g*-p(A-(L)Glu-OH)) (Liu et al. 2015), etc., have been obtained via homogeneous atom transfer radical polymerization (ATRP) of vinyl monomers, ring-opening polymerization (ROP) of aliphatic polyester monomers, and reversible addition fragmentation chain transfer polymerization (RAFT) of amino acid monomers in 1-allyl-3-methylimidazolium chloride (AmimCl), 1-butyl-3-methylimidazolium chloride (BmimCl), or DMAc/LiCl medias, which could be dispersed in water under suitable pH value or temperature conditions. However, in addition to the use of expensive ILs and DMAc/LiCl in this method, a large number of organic solvents, heavy metal catalysts and petroleum based monomers are also used, leading to a complicated and sophisticated process with high volatile organic compound (VOC) emission and difficult to separate, as well as residues of heavy metal ions depositing in resultant products. Hence, our objective is to develop a renewable, biodegradable, cost-effective, cellulose-based, waterborne biopolymer capable of forming into film having good water resistance properties.

NaOH/urea aqueous solution is a low cost and green solvent for efficiently dissolving cellulose (Cai and Zhang 2005; Pei et al. 2013; Hu et al. 2015). Generally, random flocculi without any strength could be formed when a cellulose-NaOH/urea aqueous solution is diluted by water, due to the sharp change of the micro-environment around cellulose molecules. In order to make cellulose able to be dispersed in water at room temperature in absence of NaOH and urea, chemical modification of cellulose is necessary. Gelatin, with abundant hydrophilic groups (e.g. amino and carboxyl group) to endow strong hydrophilicity, is a hydrolysate of collagen mainly composed of glutamic acid, proline and hydroxyproline (Maciejewski et al. 2017; Kirdponpattara et al. 2017; Farzamfar et al. 2017); it is expected to be introduced into the macromolecular chain of cellulose via covalent polymerization to make cellulose be self-dispersed in water, it is an effective way to realize waterborne cellulose microgel. There is little research reported on the formation of self-dispersed cellulose microgel with gelatin as a kind of macromolecular modify agent via covalent polymerization in NaOH/urea aqueous solution.

In this paper, we report a simple, low cost, and green method to chemically modify cellulose using biopolymer gelatin to prepare a new gelatin-coupled cellulose (GCC) microgel and the properties of its films. The GCC microgel obtained has more than 18% of protein bonded onto the molecular chain of cellulose and is dispersible in water. This important outcome leads to the possibility of producing water-based cellulose coatings. A cellulose-based biopolymer alternative to existing CA, NC, and petrochemical-derived acrylic coatings is thereby produced. Furthermore, a series of GCC microgels was successfully prepared in NaOH/urea aqueous solution with ECH as coupling agent via dialysis and self-dispersion pathway from aqueous medium. The effects of both the mass ratio of gelatin to cellulose (*W*/*W*) and the amount of coupling agent used on the particle size of microgel, the water resistance and contact angle of corresponding film were investigated.

Materials and methods

Materials

Cellulose (cotton linter pulps, α-cellulose ≥ 95%) was provided by Hubei Chemical Fiber Co. Ltd. (Xiangfan, China). Its viscosity-average molecular weight (Mn) was about 1.07×10^5, which was determined in a LiOH/urea aqueous solution at 25° (Cai et al. 2006). Industrial gelatin, with weight-average molecular (M_w) of 0.63×10^5 by gel permeation chromatography (GPC), was obtained from YI Weilong Biotechnology Co., Ltd. (Xiamen, China). The cellulose and gelatin were vacuum-dried for 24 h at 60 °C before use. RC dialysis membranes (100 kDa molecular weight cut off) were obtained from Yobios Bio-Tech Co. Ltd. (Xi'an, China). Epichlorohydrin (ECH, analytical grade, liquid, 1.18 g/mL), NaOH, urea were purchased from Tianli Chemical Reagents Ltd. (Tianjin, China) and used without further purification.

Preparation of self-dispersed gelatin-coupled cellulose (GCC) microgel

GCC microgel was prepared as follows: Briefly, 100 g of cellulose aqueous solution with 3 wt% in concentration was prepared by dissolving cotton linter pulps in a mixed solution of NaOH/urea/H_2O (7:12:81, by weight) at − 12 °C. A gelatin aqueous solution with the concentration of 10 wt% was obtained by dissolving 10 g of gelatin powders into 90 g of deionized water at 50 °C. Then both the cellulose and gelatin solutions were mixed and stirred immediately at room temperature for 1 h, which is needed to ensure homogeneous mixing between cellulose and gelatin, followed by adding ECH dropwisely in the blend solutions at room temperature with stirring for a desired time continuously. The reacting mixture was dialyzed against deionized water for a week (replaced water once every 6 h), using a dialysis membrane with a 100 kDa molecular weight cut off (MWCO) to remove any unreacted ECH, NaOH, urea and by-products (mainly including gelatin hydrolysates and its coupling products), and then the deionized water was added into the shredded, jelly-like substance with a vigorous stirring for 30 min to form the coarse solution of self-dispersed waterborne cellulose. Finally, the undissolved cellulose and its coupling product after the dialysis process were removed after sediment for overnight, to obtain the GCC microgel solution from the upper layer. By changing the mass ratio of cellulose to gelatin such as 90:10, 80:20, 70:30, and 60:40, a series of GCC microgels was prepared, labelled as GCC_{10}, GCC_{20}, GCC_{30} and GCC_{40}, respectively, which are listed in Table 1.

Determining the yield of water-soluble GCC microgel

In theory, three putative coupling reactions would be carried out in cellulose and gelatin solution system with ECH, which are the reactions between gelatin and gelatin (a), cellulose and cellulose (b), and gelatin and cellulose (c), respectively, as shown in Fig. S1. The yield (Y, %) of water-soluble GCC microgel is determined as the following equation:

$$Y(\%) = \frac{m_0}{3 + m_g + 3.44} \times 100$$

where m_0 is the weight of water-soluble GCC after freeze-drying; 3, m_g and 3.44 are the weight of cellulose, gelatin and ECH in the original reaction system, respectively.

Preparation of microgel films

The microgel film is obtained by casting GCC microgel solution onto a PTFE plastic plate (15 cm × 15 cm) and evaporating water at 45 °C in an oven, followed by demoulding, and then stored in a desiccator before use (50 ± 2% RH, 20 ± 1 °C).

Measurement of water resistance

Each microgel film (30 mm × 30 mm) in the dried state was immersed in deionized water at ambient temperature for a period of time, followed by wiping off the surface water with a piece of filter paper to determine the wet film weight, it was considered as a moisture equilibrium when its weight was constant. The absorbed water ratio (or the equilibrium swelling

Table 1 The particle sizes, PDI, N content (W_N, %), protein content (W_{Pro}, %) and yield (%) of GCC microgels

Series	W^a_{Gel} (%)	W^b_{Cel} (%)	n_{ECH}:n^c_{AGU}	W_N (%)	W_{Pro} (%)	Particle size (nm)	PDI	Yield (%)
Gelatin	100	0	–	14.46	90.38	8 ± 0.4	0.256 ± 0.07	–
GCC_{10}	10	90	2	2.95	18.43	147 ± 3.2	0.254 ± 0.12	18.3
GCC_{20}	20	80	2	2.99	18.69	120 ± 1.3	0.348 ± 0.09	21.3
GCC_{30}	30	70	2	3.86	24.13	87 ± 0.9	0.215 ± 0.19	35.7
GCC_{40}	40	60	2	4.93	30.81	90 ± 2.6	0.398 ± 0.24	48.6

[a] W_{Gel} = [Weight of gelatin/(Weight of cellulose + Weight of gelatin)] × 100

[b] W_{Cel} = [Weight of cellulose/(weight of cellulose + Weight of gelatin)] × 100

[c] n_{ECH}:n_{AGU} = The molar ratio of epichlorohydrin to anhydroglucose unit of cellulose

ratio, S_{eq}, g/g) of the microgel film was defined based on the formula below:

$$S = \frac{m_2 - m_1}{m_1}$$

where m_2 is the final wet weight, and m_1 is the initial weight of the dried film.

Characterization

Protein content analysis

To determine the gelatin content (W_{Pro}) in the GCC_n, the N content (W_{N}) in the microgel films was measured on an element analysis instrument (Vario EL III, Germany). The W_{Pro} value of microgel films can be calculated by:

$$W_{Pro} = W_N \times 6.25$$

Fourier transform infrared spectroscopy (FTIR)

Attenuated total reflection Fourier transform infrared spectroscopy (ATR-FTIR) spectra measurement were carried out with an FTIR spectrometer (Vertex 70, BRUKER, Germany) in the wavelength range from 4000 to 400 cm^{-1}. The samples were cut into powders and vacuum dried for 24 h, then mixed with KBr, and pressed for the measurement.

Dynamic light scattering (DLS)

The average particle size and size distribution of the microgel solutions were measured in Malvern Zetasizer ZS Instrument (dynamic light scattering, DLS). The solutions were diluted to 3 mg/mL with deionized water, followed by ultrasonic wave treatment for 20 min with a power of 75 W to form the homogenized system, then measured at 25 °C and characterized by Z-average diameter.

Gel permeation chromatography (GPC)

GPC measurement was carried out on a water-based GPC system (Waters 2695 GPC) to determine the molecular weights of GCC microgels. Samples were prepared to 3 mg/mL with 0.1 M $NaNO_3$, and obtained by filtering with 0.45 μm RC filter membrane. A series of PEG standards (M_w of 610, 4040, 16,100, 45,520, 134,300, and 298,000 Da) was used for samples and the standard curve for PEG was given in Fig. S2. Injection volume: 50 μL; mobile phase flow: 0.5 ml min^{-1}; temperature: 30 °C; run time: 25 min; mobile phase: 0.1 M $NaNO_3$.

X-ray diffraction (XRD)

XRD measurements were made using a D8 X-ray diffractometer (BRUKER, Germany) with Cu-Kα radiation(wavelength: 0.15406 nm) at a voltage of 40 kV and current of 40 mA. The 2θ diffraction diagrams were obtained between 5° and 45°.

Thermogravimetric analysis–differential scanning calorimetry (TGA–DSC)

TGA and DSC of GCC microgel films were carried out by using a STA449 thermogravimetric analyzer (BRUKER, Germany). About 3 mg of the powder samples was used for each test, the test was conducted in a nitrogen atmosphere, and the test temperature ranged from 30 to 700 °C at a gradual increase rate of 10 K min^{-1}.

Contact angle measurements

The water contact angle of the GCC microgel film was measured by using a contact angle analyzer (KRUSS, Germany), contact angles at five different places of each film sample were measured and averaged.

Scanning electron microscopy (SEM) analysis

The morphologies of the GCC microgel and its membrane were examined with a scanning electron microscopy (SEM) (FEI Quanta 600 FEG, America). A drop of microgel solution was dripped onto the copper sheet, and then the morphology was observed by spraying gold after drying. The GCC microgel membrane was frozen and sliced in liquid nitrogen to obtain the cross-section structure, then the cross-section was coated with gold and observed its morphology.

Atomic force microscopy (AFM) analysis

The surface microstructure of the microgel membrane was observed by AFM (AFM 5100, Agilent, USA).

The sample was fixed on the surface of a clean mica sheet and observed the morphology with a 2 × 2 μm scanner in dynamic mode at room temperature.

Results and discussion

Formation of self-dispersed GCC microgels

The GCC microgels are obtained by a one-step synthesis as illustrated in Scheme 1. Firstly, the homogeneous system of gelatin solution and cellulose-NaOH/urea aqueous solution are formed with non-covalent interaction, then the coupling agent ECH is added dropwisely into the blend solutions with stirring for 2 h, finally, the GCC microgels are obtained by simple dialysis, self-dispersion and separation process. The unreacted reagents, gelatin hydrolysate and its coupling product, undissolved cellulose and its coupling product had been removed (the characterization details are given in the GPC information). The N and protein contents of GCC microgels are listed in Table 1. These data show that the N content and protein content in GCC microgels increase with the increase of the gelatin content. Thus, the protein content of GCC microgels could be adjusted by changing the percent of gelatin. In addition, we also tried to directly dialyze the homogeneous system of cellulose/gelatin blend solution by distilled water to remove NaOH and urea, found cellulose flocculation and cannot be dispersed by water again. Therefore, it could be concluded by the experimental phenomena that blending could not disperse cellulose in water after the removal of cellulose solvents. Hence, we successfully achieved self-dispersed waterborne cellulose via coupling reaction of gelatin and cellulose in NaOH/urea aqueous media with ECH as a coupling agent, mainly due to the coupling agent ECH could react with –OH and $–NH_2$ to form a new functional group under the alkaline conditions (Qin et al. 2013; Navarra et al. 2015; Ciolacu et al. 2016), causing the strong H-bond within cellulose matrix can be restrained by the effect of steric hindrance and hydrophilic macromolecules, which effectively prevent the rapid aggregation of cellulose in subsequent dialysis process (Yuan et al. 2015).

It is obvious that after adding ECH, the gelatin solution and cellulose-NaOH/urea system became very complex. Among them, gelatin and gelatin, cellulose and cellulose, and gelatin and cellulose could be coupled by ECH, respectively. In order to prove that the reaction in this complex system was performed as expected, the molecular weight of the possible reaction products were measured firstly by GPC. Figure 1 shows the GPC diagrams of gelatin, gelatin treated in NaOH/urea aqueous media at the absence of cellulose and epichlorohydrin (Gel-NaOH/

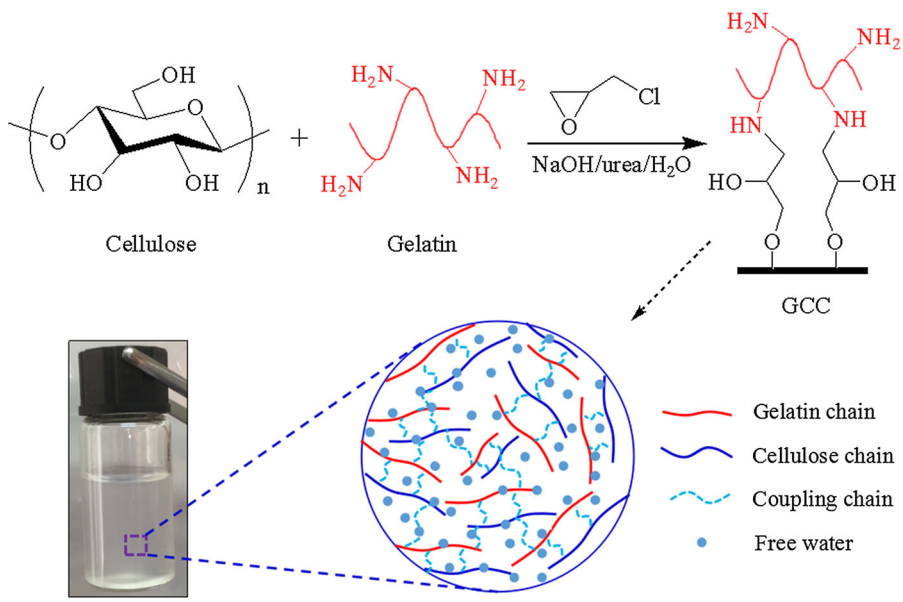

Scheme 1 Chemical reaction equation of the coupling reaction between cellulose and gelatin in NaOH/urea aqueous solution using ECH

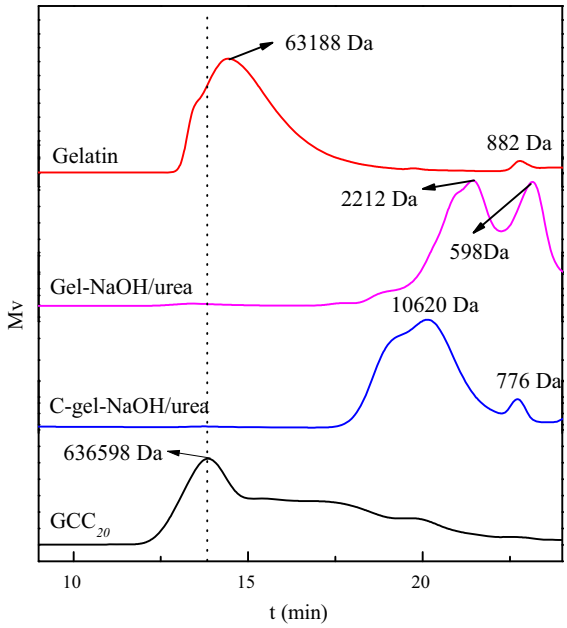

Fig. 1 The GPC elution diagrams of native gelatin, Gel-NaOH/urea, C-gel-NaOH/urea, and GCC_{20}

urea), ECH-coupled gelatin in NaOH/urea aqueous media (C-gel-NaOH/urea) at the absence of cellulose, and GCC_{20}. The average molecular weights of gelatin, Gel-NaOH/urea, C-gel-NaOH/urea, and GCC_{20} are 0.88–63.19, 0.60–2.21, 0.78–10.62 and 636.60 kDa, respectively (Table 2). In the elution diagram of native gelatin, the average molecular weight is composed of polypeptide and small amino acids. Obviously, the mean molecular weight of gelatin dramatically decreased after treated in NaOH/urea aqueous media due to hydrolysis, however, the molecular weight of hydrolyzed gelatin increased via the coupling action of ECH, and the molecular weight was up to 10.62 kDa from homocoupling reaction. In the diagram of GCC_{20}, it is clearly exhibited a left shift of the molecular weight of 636.60 kDa with a narrow PDI at short time, which is much higher than that of gelatin and C-gel-NaOH/urea, indicating new polymer is formed from coupling polymerization of cellulose and gelatin. The MWCO of the dialysis membrane used in this work is 100 kDa, therefore, it is believed that the gelatin hydrolysate and its coupling product can be removed during dialysis process, to get the GCC microgel as desired. As exhibited in Table 1, the yield of GCC microgels increased with the increase of gelatin content, which was probably attributed to the more gelatin hydrolysates were conductive to the collision between –OH of cellulose and $–NH_2$ of gelatin to promote the coupling reaction, leading to the more hydrolyzed gelatin molecules were bonded onto the cellulose backbone.

Table 2 Summary of number- and weight-average molecular weight (Mn and Mw) and polydispersity index (PDI) of gelatin, Gel-NaOH/urea, C-gel-NaOH/urea, and GCC_{20} measured by GPC

	Mn (kDa)	Mw (kDa)	PDI
Gelatin	0.80–17.74	0.88–63.19	3.561
Gel-NaOH/urea	0.58–1.62	0.60–2.21	1.364
C-gel-NaOH/urea	0.73–3.69	0.78–10.62	2.879
GCC_{20}	627.19	636.60	1.015

Figure 2 shows the FTIR spectra of cellulose, gelatin, and GCC_n samples. From the spectrum of gelatin, the peaks at 1634 and 1535 cm^{-1} are ascribed to carbonyl groups (amide I and amide II bands) (Ooi et al. 2015). These absorption peaks at 3343, 2896, 1428, 1104 and 1024 cm^{-1} are ascribed to characteristic bands of cellulose, and they are attributed to O–H and C–H stretching vibrations, C–H bending vibrations of methylene and methenyl-, C–O–C stretching vibration bands (Zhang et al. 2018a, b), respectively. In comparison with that of gelatin, the FTIR spectra of GCC_n apparently have two new peaks at 3343 and 1030 cm^{-1} attributed to O–H and C–O–C groups of

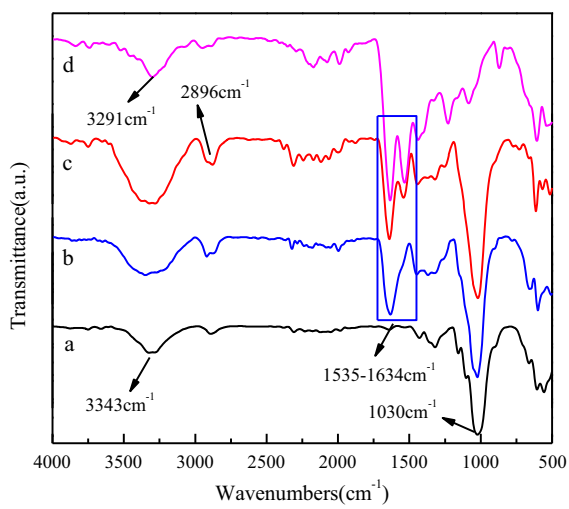

Fig. 2 FTIR spectra of cellulose (*a*), GCC_{20} (*b*), GCC_{40} (*c*), and gelatin (*d*)

cellulose, respectively, which demonstrates the peptide chains of gelatin are successfully coupled with the glucose chain of cellulose, because the undissolved cellulose and its coupled product could form precipitation and be removed under dialysis, self-dispersion and separation process. Moreover, the characteristic peaks at 3343 cm^{-1} (–OH stretching) and 3291 cm^{-1} (–NH_2 stretching) for the GCC_n become broaden, mostly owed to the –NH_2 groups and –OH groups having reacted with epoxy groups from ECH. Especially compared to cellulose, the intensities of the peaks for the C–O–C (1024–1104 cm^{-1}), C–H (2896 cm^{-1}) and –CH_2 (1428 cm^{-1}) increase obviously in GCC microgels because the coupling agent ECH can provide abundant C–O–C, C–H and –CH_2 groups (Zhao et al. 2016). These changes further indicate the successful coupling occurred between cellulose and gelatin. Consequently, from the results of element analysis, GPC and FTIR, the peptide chain is successfully conjugated to the backbone of cellulose, and the average molecular weight of microgel is up to 636.60 kDa.

Particle size analysis for GCC microgels

To prepare good dispersivity and homogeneous particle size of GCC microgels, a series of microgels is prepared with different gelatin and ECH content. As shown in Table 1, GCC microgel has a smaller particle size with the increase of the amount of protein introduced; when the protein content is higher than 24%, the average particle size of microgel has a smaller particle size with the increase of the amount of protein introduceds is about 88 nm, mainly because the increase of gelatin content might lead to greater contact probability between the peptide chain of gelatin and –OH of cellulose glucose unit, which promotes reaction efficiency (Pei et al. 2015) and increases the effect of steric hindrance, and the number of hydrophilic macromolecules on the cellulose glucose chain are also increased, improving dispersibility of GCC microgel in water.

Table 3 shows the effect of the amount of coupling agent on the particle sizes of microgels. It is found that, when the coupling agent ECH to anhydroglucose unit (AGU) of cellulose molar ratio is below 2:1, the formation of self-dispersed GCC microgels is not conducive due to its decreased hydrophilic gelatin content, while strong H-bond interaction, drastic aggregation, and crystallization of cellulose exert primary influences on waterborne cellulose microgel. The cellulose matrix coupled with gelatin grafting reaction could be self-dispersed in water when the molar ratio of ECH to AGU varies from 2:1 to 4:1. With the increases of ECH molar ratio, the amorphous regions and hydrophilic groups (i.e. –NH_2 and –COOH) dominate the water uptake capability due to the increasing of coupling degree between gelatin and cellulose. In addition, introducing gelatin leads to the formation of long peptide chains, facilitating the formation of tight structures and higher curl degree (Wang et al. 2017), the GCC_{40} microgel has Z-average particle size of approximate 83 nm with the molar ratio of ECH to AGU of 3:1 (Fig. 3a). SEM image of microgel is illustrated in Fig. 3b and shows well-dispersed whisker-like nanoparticle with average length of 120 nm and width of 10 nm, respectively. The observed particle size is slightly higher than that of the DLS result. The difference may be due to the different states of sample during analysis. Typically, the DLS technique is designed to measure the hydrodynamic diameter of spherical particles, while the SEM image test is carried out under the dry state and likely aggregation under dry process. Moreover, as ECH is excess (above 3:1), it becomes unfavorable to the absorption of water instead because much reticular structure, and too much hydroxyl groups and amino groups are consumed, while the increase of ECH leads to higher coupling density in the macromolecular chains (Zhao et al. 2016), so it is difficult to disperse polymer, as to particle size increases. However, further adding the amount of ECH causes the formation of solid-like (weak hydrogel), indicating that excessive coupling agent accelerates the coupling of cellulose and gelatin, resulting in the gel. The above results show that GCC microgels with good dispersivity and homogeneous particle size can be obtained by adjusting the molar ratio of ECH to AGU is not less than 2:1 and the incorporation of gelatin as long as $W_{Gel} \geq 20$ wt%.

In order to confirm the stability of GCC microgels, the changes of particle size of GCC_{20} and GCC_{40} microgels with the storage duration are measured and shown in Fig. 3c. There are no obvious changes in the particle sizes of microgels after 90 days, indicating that this kind of microgels could be stable in storage for more than three months. The cellulose and gelatin

Table 3 Effect of ECH content on particle size of GCC_{40} microgel

	ECH/AGU = 1:1	ECH/AGU = 2:1	ECH/AGU = 3:1	ECH/AGU = 4:1
Size (d nm)	–	90 ± 2.6	83 ± 2.2	105 ± 4.3
PDI	–	0.398 ± 0.24	0.153 ± 0.40	0.225 ± 0.34

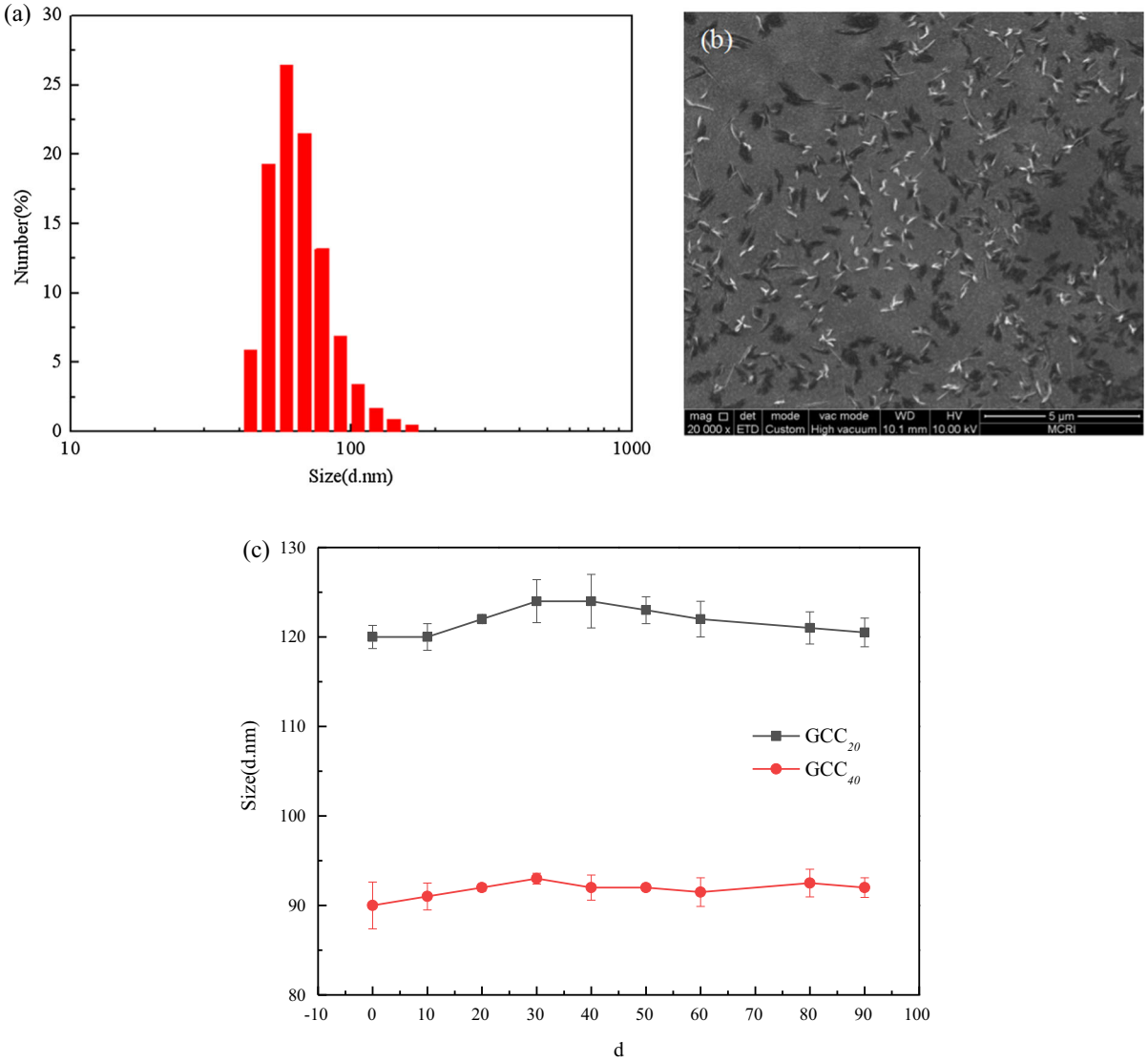

Fig. 3 **a** Particle size distribution of GCC_{40} microgel; **b** the morphology of GCC_{40} microgel by SEM; **c** effect of storage time on the particle sizes of GCC_{20} and GCC_{40} microgels (the Mw of GCC_{20} and GCC_{40} is 636.60 and 651.49 kDa, respectively)

chains are connected via covalent bonding, there will be neither transition from microgel structure to molecular chain structure nor aggregation occured. Furthermore, the greater molecular weight of microgel, the more stable the dispersion, this agrees with Guo's report (Guo et al. 2012).

XRD analysis of film

The XRD patterns of native cellulose (cotton linter pulp), gelatin and GCC_n microgel films are shown in Fig. 4. Cellulose exhibits four obvious diffraction peaks at 2θ = 14.9°, 16.5°, 22.9° and 34.4°, normally assigned to the (1–10), (110), (200), and (004) planes of cellulose type I, respectively (French 2014). For gelatin, the peak located at about 2θ = 8.6° is based on the inter-helix distance of the triple helix of gelatin, and a broad diffraction peak at 2θ = 21.7° typical of the amorphous fraction of gelatin. Such peaks are similar to the results from previously reports (Quero et al. 2015, 2018). For the XRD patterns of GCC_{20} and GCC_{40} films, it is obvious that the peak centered at 2θ = 8.6° corresponding to the characteristic peak of gelatin is identified, and the peak at 2θ = 21.7° for gelatin may be overlapped with that of modified cellulose when gelatin is bonded onto the molecular chain of cellulose, while none of the diffraction peaks of cellulose can be observed in the diffraction patterns of GCC_n films, but a new broad peak at 2θ = 20.2° is found. Since the cellulose pattern is from the original linters pulp and not from the dissolved cellulose that did not get mixed with the gelatin, and the gelatin has intensity in the 20° region, the band at ∼ 20° for GCC_n may be that the cellulose somehow encourages crystallization of the gelatin. The above results demonstrate that the original crystalline structure of cellulose had been disrupted after being coupled with gelatin.

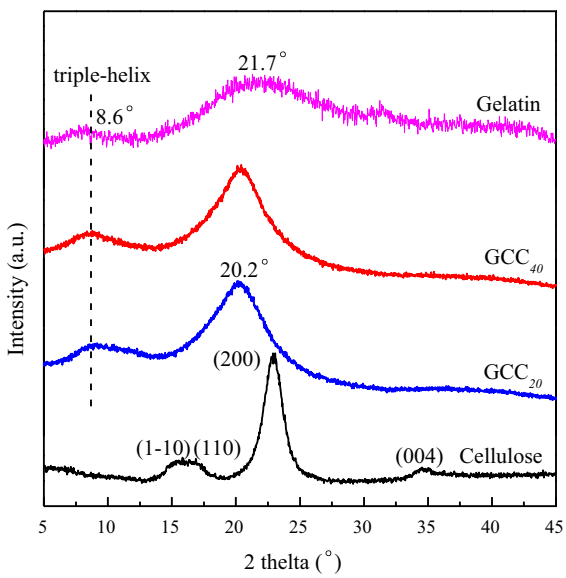

Fig. 4 X-ray diffraction patterns of native cellulose, GCC_{20}, GCC_{40}, and gelatin

TGA–DSC analysis of the films

The thermal properties of cellulose, gelatin, and GCC_{20} microgel films in N_2 atmosphere are investigated using TGA, DTG and DSC as shown in Fig. 5. The thermal degradation process of films consisted of two stages and the first peak is related to the evaporation of bound water nothing to do with the thermal degradation temperature of polymers, so we did not analyze the first stage in the TGA curves. The degradation in the second stage of gelatin film starting at 216 °C (T_0) with a maximum mass losses at 312 °C (T_m) were due to the degradation of polypeptide chain. T_0 at 288 °C with T_m of 358 °C in the second stage of cellulose were observed and related to the cleavage of glucoside bonds and hydrogen bonds during the processes of demethoxylation and dehydration (Yang et al. 2009). In the TGA curve of GCC_{20}, the second stage started at 228 °C with T_m of 328 °C, both of which were lower than those of cellulose. Hence, it is indicated that the hydrogen bond and crystalline structure of cellulose have been destroyed with the introduction of gelatin which is consistent with the XRD results.

The DSC thermograms of films are described in Fig. 5c, d. There is a decomposition endothermic peak of phase transition at 319 °C and a wide charring endotherm at between 500–590 °C for cellulose, respectively, showing a corresponding to the final decomposition temperature of leaving 10% charred residue at 584 °C for cellulose (Jiang and Hsieh 2016; Ma et al. 2018). Gelatin shows a wide endothermic melting peak at temperature in the range of 112–123 °C, which is generally related to the disruption of ordered phases of gelatin. Such result is similar to one reported in other study (Theerawitayaart et al. 2019). However, in the endothermic curve of GCC microgel, the endothermic peak of gelatin and phase transition at 319 °C of cellulose disappeared, this indicates that the structure of cellulose had changed greatly after being coupled with gelatin. Moreover, the shoulder peak at 370 °C is mainly belonged to the rupture of the C–N bonds, and a heat absorption peak at 489 °C for charring tends to shift to the lower temperature. This further demonstrates that the

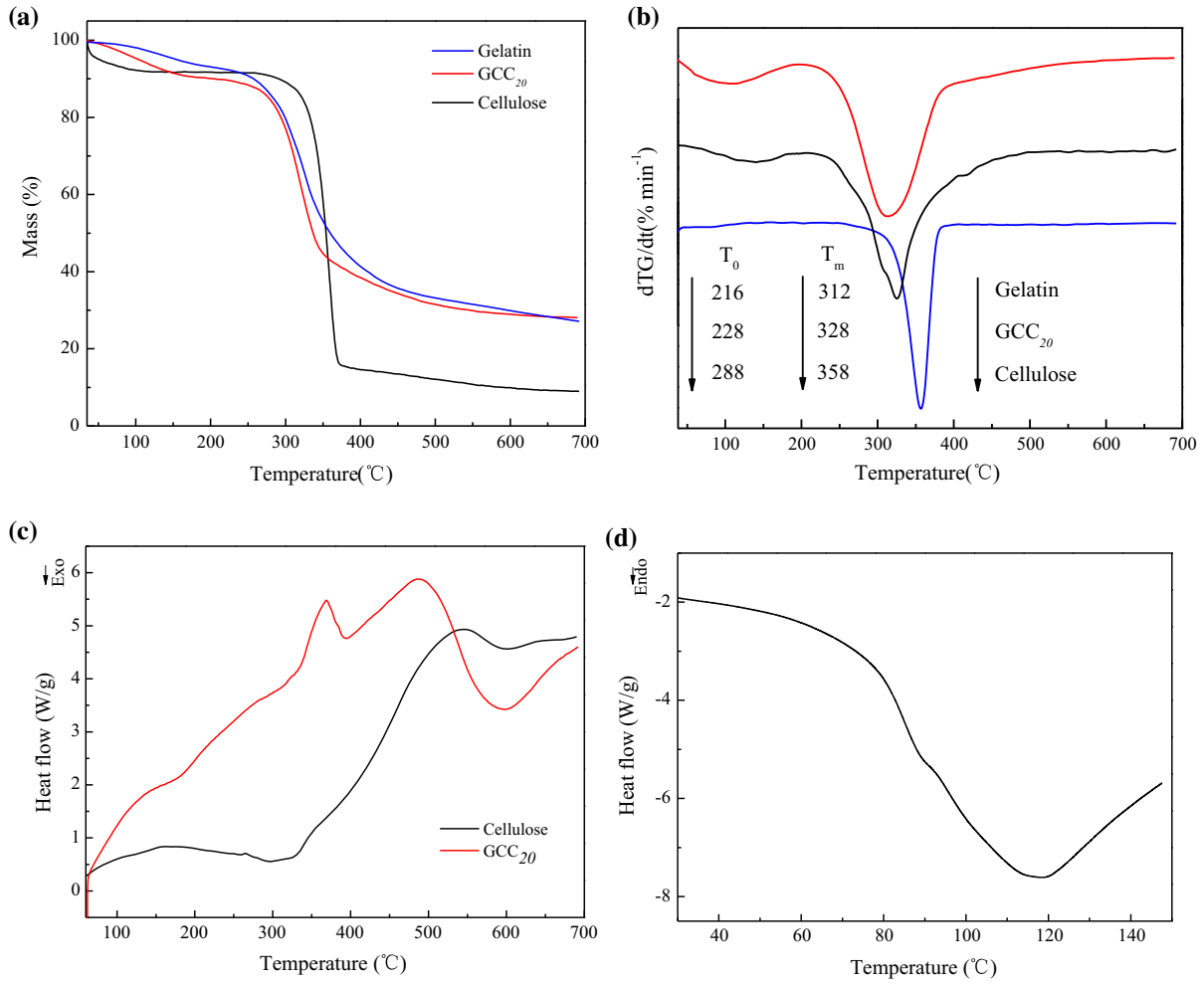

Fig. 5 TGA (**a**) and DTG (**b**) of gelatin, GCC_{20} and cellulose; DSC of GCC_{20} and cellulose (**c**) and gelatin (**d**). Where T_0 is the starting point of decomposition, and T_m is the temperature with maximum decomposition rate

hydrogen bond and crystalline structure of cellulose have been destroyed. However, in comparison with existing water-soluble hydroxypropyl methylcellulose (HPMC) (Ding et al. 2015; Karlsson et al. 2015), the T_m and thermal decomposition endothermic temperature of these GCC microgel films are higher, indicating the GCC microgel films exhibit excellent heat-resistance.

Contact angle and water resistance measurements of GCC microgel film

Generally, the regenerated cellulose and native gelatin films possess a high water sensitivity (Eriksson et al. 2005; Banerjee et al. 2009), which are not desirable for application in wet state. Figure 6a shows the average contact angle of native gelatin and GCC_n films. The gelatin films present low contact angle of about 55° due to the presence of hydrophilic groups (Eriksson et al. 2005; Banerjee et al. 2009). With the increasing of gelatin content in GCC microgel, the contact angle of the GCC microgel films decreases; however, the values of the microgel films in this work are much higher than those of the water-soluble cellulose derivative (e.g. HEC, HPC, and HPMC, etc.) and HPMC/protein composite films reported previously (Karlsson et al. 2015; Ding et al. 2015), suggesting the surface hydrophobicity of the microgel films is obviously improved. This may be attributed to the reassociate inside the molecules and the network

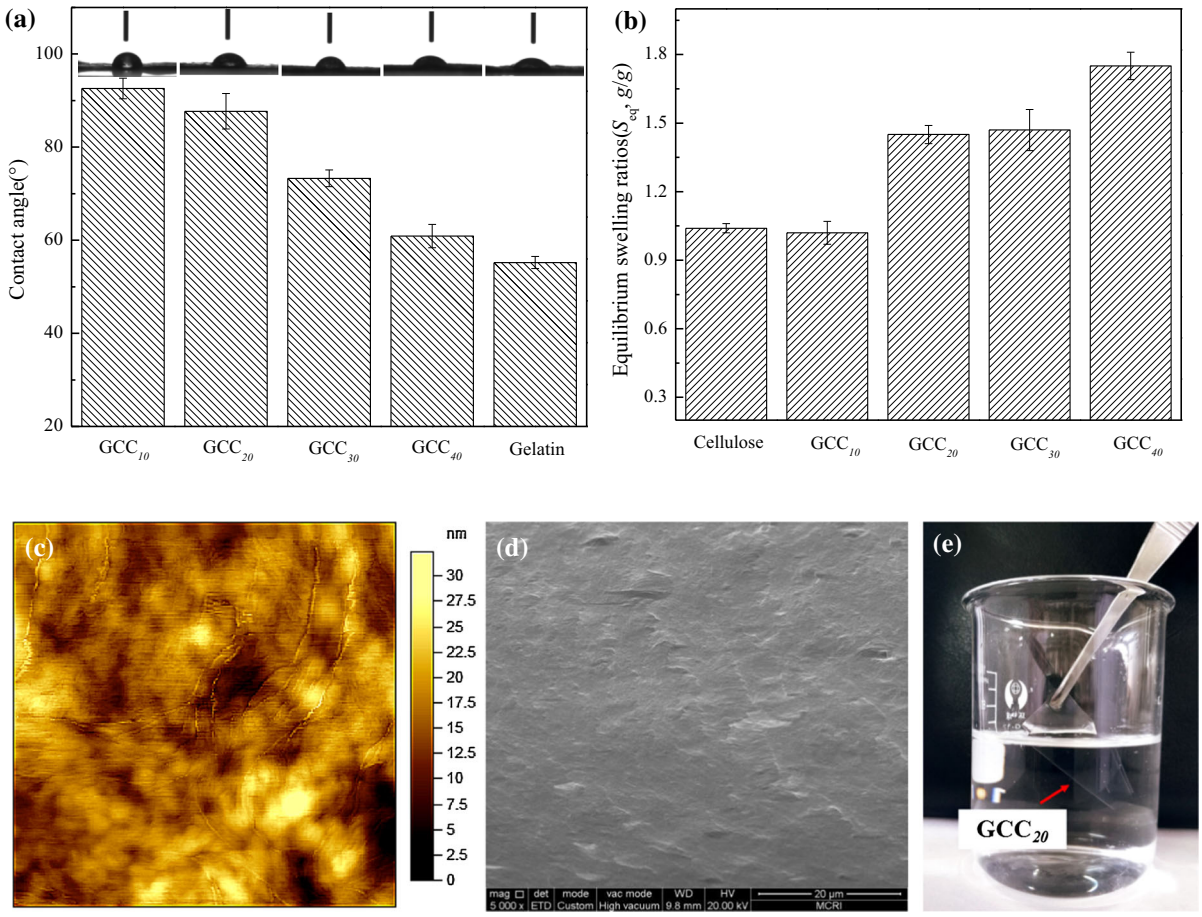

Fig. 6 Contact angle (**a**) and swelling behavior (**b**) of GCC microgel films with different content of gelatin; AFM surface (**c**) and SEM cross-section (**d**) images of GCC_{20} film; (**e**) Photograph of water resistance of dry GCC_{20} film after soaking in deionized water for 24 h

formed between cellulose and gelatin chains during the drying process, meanwhile, the more hydrophilic groups are closed in the structure reduce the binding capacity with water. The results indicate that the coupling reaction has effectively enhanced the water resistance of films. In order to further study how the gelatin content affects the water resistance of GCC_n films, their swelling behaviors are investigated. Figure 6b illustrates the equilibrium swelling ratios of GCC_n films. The breakup of native gelatin film in deionized water occurs at 15 min after it is immersed and completely dissolves after 1 h. The water uptake ratio for the GCC_n films increase as the gelatin content increases due to the strong hydrophilic property of gelatin, but GCC microgel films are only in the swelling state after it is immersed in the water for 24 h, owing mainly to the covalent interaction obviously increases molecular weight of polymers, and the network structure in GCC_n film systems formed effectively via intermolecular chemical coupling, which prevents free-chain movement ability of cellulose and gelatin, leading to the water resistance of the GCC_n films increase. Another possible reason of strong water resistance is that the microgels exhibit a strong self-assembly ability which make film-formation to present a homogeneous and compact structure, reducing the binding capacity with water. Figure 6c, d present the AFM surface and SEM cross-section images of GCC_{20} film, respectively. As shown in Fig. 6c, the film exhibits a flat and uniform surface, the corresponding roughness is 3 nm which calculated by the system-provided software. It could be seen from SEM image that the GCC_{20} film presents a compact cross-section structure, indicating the good compatibility among GCC microgel film. The uniform and dense structure endows the microgel film with

excellent hydrophobicity and water resistance. Figure 6e displays photograph of the water resistance of dry GCC_{20} film after soaking in deionized water for 24 h, which still remains flawless and perfect. However, the existing water-soluble cellulose derivative films (e.g. HPC, HEC, HPMC, etc.) are easy to be dissolved in water (Karlsson et al. 2015; Ding et al. 2015).

Conclusions

A water-soluble GCC microgel is successfully obtained by the incorporation of gelatin into cellulose with epichlorohydrin (ECH) as a coupling agent in NaOH/urea aqueous solution. The particles of GCC microgels show uniform size and high stability. Elemental analysis, GPC and FTIR indicate that gelatin has been successfully incorporated into the glucose chain of cellulose, and molecular weight of GCC microgel with narrow PDI of 1.015 is up to 636.60 kDa. XRD proves the crystallinity of cellulose decreased by coupling with gelatin, accompanying with larger amorphous region. TGA and DSC results confirm that microgel films display high thermal stability properties. The microgel films exhibit more stronger water resistance than the existing water-soluble cellulose derivatives owing to the intermolecular chemical coupling. In this work, a new biopolymer based on cellulose and gelatin has been realized in nonorganic solvent, and the problem that cellulose cannot be dispersed in water is also solved. The film obtained from microgel would bring wide application prospect in the field of coating, packaging and bio-film materials.

Acknowledgments This work was supported by the Hongliang Research Fund (413118) and Doctor Research Fund of Shaanxi University of Science and Technology.

References

Banerjee I, Mishra D, Maiti T (2009) PLGA microspheres incorporated gelatin scaffold: microspheres modulate scaffold properties. Int J Biomater 2009:1–9

Cai J, Zhang L (2005) Rapid dissolution of cellulose in LiOH/Urea and NaOH/Urea aqueous solutions. Macromol Biosci 5:539–548

Cai J, Liu Y, Zhang L (2006) Dilute solution properties of cellulose in LiOH/urea aqueous system. J Polym Sci Part B Polym Phys 44:3093–3101

Ciolacu D, Rudaz C, Vasilescu M, Budtova T (2016) Physically and chemically cross-linked cellulose cryogels: structure, properties and application for controlled release. Carbohyd Polym 151:392–400

Ding C, Zhang M, Li G (2015) Preparation and characterization of collagen/hydroxypropyl methylcellulose (HPMC) blend film. Carbohyd Polym 119:194–201

Duan H, Shao Z, Zhao M, Zhou Z (2016) Preparation and properties of environmental-friendly coatings based on carboxymethyl cellulose nitrate ester & modified alkyd. Carbohyd Polym 137:92–99

Eriksson J, Malmsten M, Tiberg F, Callisen T, Damhus T (2005) Enzymatic degradation of model cellulose films. J Colloid Interface Sci 284(1):99–106

Esteghlal S, Niakosari M, Hosseini S, Mesbahi G, Yousefi G (2016) Gelatin-hydroxypropyl methylcellulose water-in-water emulsions as a new bio-based packaging material. Int J Biol Macromol 86:242–249

Farzamfar S, Naseri N, Vaez A, Esmaeilpour F, Ehterami A, Sahrapeyma H (2017) Neural tissue regeneration by a gabapentin-loaded cellulose acetate/gelatin wet-electrospun scaffold. Cellulose 25(2):1229–1238

French A (2014) Idealized powder diffraction patterns for cellulose polymorphs. Cellulose 21:885–896

Ge W, Guo Y, Zhong H (2015) Synthesis, characterization and micellar behaviors of hydroxyethyl cellulose-graft-poly(lactide/e-caprolactone/p-dioxanone). Cellulose 22(4):2365–2374

Geng H (2018) A one-step approach to make cellulose-based hydrogels of various transparency and swelling degrees. Carbohyd Polym 186:208–216

Guo Y, Wang X, Shu X, Shen Z, Sun R (2012) Self-assembly and paclitaxel loading capacity of cellulose-graft-poly(lactide) nanomicelles. J Agric Food Chem 60(15):3900–3908

Guo Y, Wang X, Shen Z, Shu X, Sun R (2013) Preparation of cellulose-graft-poly(ε-caprolactone) nanomicelles by homogeneous ROP in ionic liquid. Carbohyd Polym 92(1):77–83

Hu H, You J, Gan W, Zhou J, Zhang L (2015) Synthesis of allyl cellulose in NaOH/urea aqueous solutions and its thiol-ene click reactions. Polym Chem 6:3543–3548

Ifuku S, Kadla JF (2009) Preparation of a thermosensitive highly regioselective cellulose/N-isopropylacrylamide copolymer through atom transfer radical polymerization. Biomacromolecules 9(11):3308–3313

Jiang F, Hsieh Y (2016) Self-assembling of TEMPO oxidized cellulose nanofibrils as affected by protonation of surface carboxyls and drying methods. ACS Sustain Chem Eng 4:1041–1049

Karlsson K, Schuster E, Stading M, Rigdahl M (2015) Foaming behavior of water-soluble cellulose derivatives: hydroxypropyl methylcellulose and ethyl hydroxyethyl cellulose. Cellulose 22(4):2651–2664

Kirdponpattara S, Phisalaphong M, Kongruang S (2017) Gelatin-bacterial cellulose composite sponges thermally cross-linked with glucose for tissue engineering applications. Carbohyd Polym 177:361–368

Klemm D, Heublein B, Fink H, Bohn A (2005) Cellulose: faszinierendes biopolymer und nachhaltiger rohstoff. Angew Chem 117(22):3422–3458

Liu Y, Jin X, Zhang X, Han M, Ji S (2015) Self-assembly and chiroptical property of poly(N-acryloyl-L-amino acid) grafted celluloses synthesized by RAFT polymerization. Carbohyd Polym 117:312–318

Lu Y, Yuan W (2018) Superhydrophobic three-dimensional porous ethyl cellulose absorbent with micro/nano-scale hierarchical structures for highly efficient removal of oily contaminants from water. Carbohyd Polym 191:86–94

Ma S, Song G, Feng N (2012) Preparation and characterization of self-emulsified waterborne nitrocellulose. Carbohyd Polym 89:36–40

Ma Y, Zhou G, Ding J, Li S, Wang G (2018) Preparation and characterization of an agglomeration-cementing agent for dust suppression in open pit coal Mining. Cellulose 25:4011–4029

Maciejewski B, Weitschies W, Schneider F, Sznitowska M (2017) Gastroresistant gelatin films prepared by addition of cellulose acetate phthalate. Pharmazie 72(6):324–328

Navarra M, Bosco C, Moreno J, Vitucci F, Paolone A, Panero S (2015) Synthesis and characterization of cellulose-based hydrogels to be used as gel electrolytes. Membranes 5(4):5810–5823

Ooi S, Ahmad I, Amin M (2015) Cellulose nanocrystals extracted from rice husks as a reinforcing material in gelatin hydrogels for use in controlled drug delivery systems. Ind Crops Prod 93:227–234

Pei Y, Yang J, Liu P, Xu M, Zhang X, Zhang L (2013) Fabrication, properties and bioapplications of cellulose/collagen hydrolysate composite films. Carbohyd Polym 92:1752–1760

Pei Y, Ye D, Zhao Q, Wang X, Zhang C (2015) Effectively promoting wound healing with cellulose/gelatin sponges constructed directly from a cellulose solution. J Mater Chem B 3:7518–7528

Qi H, Liebert T, Meister F, Heinze T (2009) Homogenous carboxymethylation of cellulose in the NaOH/urea aqueous solution. React Funct Polym 69:779–784

Qin X, Lu A, Zhang L (2013) Gelation behavior of cellulose in NaOH/urea aqueous system via cross-linking. Cellulose 20:1669–1677

Qiu X, Tao S, Ren X, Hu S (2012) Modified cellulose films with controlled permeatability and biodegradability by crosslinking with toluene diisocyanate under homogeneous conditions. Carbohyd Polym 88:1272–1280

Quero F, Coveney A, Lewandowska A, Richardson R, Calderón P, Lee K, Eichhorn S, Alam M, Enrione J (2015) Stress transfer quantification in gelatin-matrix natural composites with tunable optical properties. Biomacromolecules 16:1784–1793

Quero F, Padilla C, Campos V, Luengo J, Caballero L, Melo F, Li Q, Eichhorn S, Enrione J (2018) Stress transfer and matrix-cohesive fracture mechanism in microfibrillated cellulose-gelatin nanocomposite films. Carbohyd Polym 195:89–98

Song Y, Sun Y, Zhang X, Zhou J, Zhang L (2008) Homogeneous quaternization of cellulose in NaOH/Urea aqueous solutions as gene carriers. Biomacromolecules 9:2259–2264

Su X, Zhao Q, Zhang D, Dong W (2015) Synthesis and membrane performance characterization of self-emulsified waterborne nitrocellulose dispersion modified with castor oil. Appl Surf Sci 356:610–614

Su X, Zhang Y, Zhao D, Chen Z (2017) Synthesis and characterization of carboxylate waterborne cellulose emulsion based on cellulose acetate. Cellulose 24(5):1–9

Sui X, Yuan J, Zhou M, Zhang J, Yang H (2008) Synthesis of cellulose-graft-poly(N,N-dimethylamino-2-ethyl methacrylate) copolymers via homogeneous ATRP and their aggregates in aqueous media. Biomacromolecules 9(10):2615–2620

Sun N, Wang T, Yan X (2017) Self-assembled supermolecular hydrogel based on hydroxyethyl cellulose: formation, in vitro release and bacteriostasis application. Carbohyd Polym 172:49–59

Suzuki T, Kono K, Shimomura K, Minami H (2014) Preparation of cellulose particles using an ionic liquid. J Colloid Interface Sci 418:126–131

Theerawitayaart W, Prodpran T, Benjakul S, Sookchoo P (2019) Properties of films from fish gelatin prepared by molecular modification and direct addition of oxidized linoleic acid. Food Hydrocolloids 88:291–300

Tristram CJ, Mason JM, Williams DB, Hinkley SF (2015) Doubly renewable cellulose polymer for water-based coatings. ChemSusChem 8(1):63–66

Wang B, Lv X, Chen S, Li Z, Yao J (2017) Bacterial cellulose/gelatin scaffold loaded with VEGF-silk fibroin nanoparticles for improving angiogenesis in tissue regeneration. Cellulose 24(11):5013–5024

Xia G, Wan J, Zhang J, Zhang X, Xu L, Wu J (2016) Cellulose-based films prepared directly from waste newspapers via an ionic liquid. Carbohyd Polym 151:223–229

Xu F, Zhu Y, Liu F, Nie J, Ma J (2010) Comb-shaped conjugates comprising hydroxypropyl cellulose backbones and low-molecular-weight poly(N-isopropylacryamide) side chains for smart hydrogels: synthesis, characterization, and biomedical applications. Bioconjug Chem 21(3):456–464

Yang Q, Lv A, Qi H, Sun Y, Zhang X, Zhang L (2009) Properties and bioapplications of blended cellulose and corn protein films. Macromol Biosci 9:849–856

Yang X, Liu G, Peng L, Guo J, Tao L (2017) Highly efficient self-healable and dual responsive cellulose-based hydrogels for controlled release and 3D cell culture. Adv Func Mater 27(40):1–10

You J, Zhao L, Wang G, Zhou H, Zhou J, Zhang L (2014) Quaternized cellulose-supported gold nanoparticles as capillary coatings to enhance protein separation by capillary electrophoresis. J Chromatogr A 1343:160–166

Yuan Z, Zhang J, Jiang A, Lv W, Wang Y, Geng H (2015) Fabrication of cellulose self-assemblies and high-strength ordered cellulose films. Carbohyd Polym 117:414–421

Zhang X, Weeks BL (2014) Preparation of sub-micron nitrocellulose particles for improved combustion behavior. J Hazard Mater 268:224–228

Zhang X, Liu X, Zheng W, Zhu J (2012) Regenerated cellulose/graphene nanocomposite films prepared in DMAC/LiCl solution. Carbohyd Polym 88:26–30

Zhang D, Zhang N, Song P, Hao J, Wan Y (2018a) Functionalized cellulose beads with three dimensional porous

structure for rapid adsorption of active constituents from Pyrola incarnata. Carbohyd Polym 181:560–569

Zhang Y, Jiang Y, Han L, Wang B, Xu H (2018b) Biodegradable regenerated cellulose-dispersed composites with improved properties via a pickering emulsion process. Carbohyd Polym 179:86–92

Zhao Y, He M, Zhao L, Wang S, Li Y (2016) Epichlorohydrin-cross-linked hydroxyethyl cellulose/soy protein isolate composite films as biocompatible and biodegradable implants for tissue engineering. ACS Appl Mater Interfaces 8:2781–2795

Zhou J, Zhang L, Deng Q, Wu X (2004) Synthesis and characterization of cellulose derivatives prepared in NaOH/Urea aqueous solutions. J Polym Sci Part A Polym Chem 42:5911–5920

Zhou J, Qin Y, Liu S, Zhang L (2006) Homogenous synthesis of hydroxyethylcellulose in NaOH/Urea aqueous solution. Macromol Biosci 6:84–89

Zhou J, Xu Y, Wang X, Qin Y, Zhang L (2008) Microstructure and aggregation behavior of methylcelluloses prepared in NaOH/urea aqueous solutions. Carbohyd Polym 74:901–906